Local Distortion Induced Metal-to-Insulator Phase Transition in $PrRu_4P_{12}$

D. Cao,[1] R. H. Heffner,[1] F. Bridges,[2] I.-K. Jeong,[1] E. D. Bauer,[1] W. M. Yuhasz,[3] and M. B. Maple[3]

[1]*Los Alamos National Laboratory, MS-K764, Los Alamos, New Mexico 87545, USA*

[2]*Physics Department, University of California, Santa Cruz, California 95064, USA*

[3]*Department of Physics and Institute for Pure and Applied Physical Science, University of California, San Diego, LaJolla, California 92093, USA*

(Received 31 August 2004; published 24 January 2005)

Extended x-ray absorption fine structure (EXAFS) experiments have been carried out on $PrRu_4P_{12}$ and $PrOs_4P_{12}$ to study the metal-to-insulator (MI) phase transition in $PrRu_4P_{12}$. No Pr displacement was observed across the MI transition temperature from the EXAFS data. Instead, our EXAFS data clearly show that a Ru displacement is associated with this MI transition. The very high Debye temperature for the Ru-P bond ($\Theta_D = 690$ K) suggests that a slight rotation/displacement of relatively rigid RuP_6 octahedra leads to this small Ru displacement, which accompanies the MI transition at 62 K in $PrRu_4P_{12}$.

DOI: 10.1103/PhysRevLett.94.036403 PACS numbers: 71.30.+h, 61.10.Ht

The filled skutterudites have generated significant interest due to a broad range of novel physical properties, which include unconventional superconductivity, heavy fermion, and non-Fermi liquid behavior, as well as their potential thermoelectric applications in industry. Transport measurements show that most of these materials are metals with a very poor thermal conductivity, with several phosphide skutterudites (such as $CeFe_4P_{12}$ and $CeRu_4P_{12}$) being semiconductors instead [1,2]. Despite theoretical attempts to calculate the band structure of the filled skutterudites, a good understanding of the semiconducting behavior in these phosphides is still lacking.

Recently, $PrRu_4P_{12}$ was found to have a metal-to-insulator (MI) phase transition near T_{MI} of $\sim$62 K [3]. Magnetic susceptibility and x-ray diffraction measurements [3] by Sekine *et al.* suggested that this MI transition is neither magnetic nor crystallographic in origin. Although valence fluctuations of the Pr ion might lead to this MI transition, a detailed x-ray absorption near edge structure (XANES) study of the Pr L_{II} edge for $PrRu_4P_{12}$ suggested that the Pr valence stays at 3^+ above and below T_{MI} [4]. Recent electron diffraction experiments by Lee *et al.* showed weak superlattice spots at 12 and 40 K, which were not observed at 70 K [5]. The observation was then attributed to a structural phase transition from $Im\bar{3}$ to another cubic phase, $Pm\bar{3}$, as temperature decreases from 70 to 40 K. In the $Pm\bar{3}$ phase, the Ru atoms are displaced along (1, 1, 1) directions. It was also suggested theoretically by Curnoe *et al.* that a symmetry lowering (1, 1, -2) Ru displacement leading to a *Pmmm* phase may be responsible for this MI transition, though a (1, 1, 1) distortion mode leading to a $Pm\bar{3}$ phase could not be excluded [6,7]. Band structure calculations also showed that a very tiny P distortion could open a band gap at the Fermi surface, leading to the MI phase transition in $PrRu_4P_{12}$ [8].

Despite many experimental and theoretical studies of $PrRu_4P_{12}$ indicating that a structural distortion is responsible for the MI transition, there is still a lack of clear experimental evidence, which hinders a deeper understanding of this phenomenon. The main problem is that any structural distortion associated with the MI transition has to be very small, so that typical diffraction techniques cannot definitively observe it. Although recent synchrotron x-ray diffraction experiment on a single crystal $PrRu_4P_{12}$ suggested a $Pm\bar{3}$ phase at 10 K [9], no high-T data were reported for comparison purposes. The extended x-ray absorption fine structure (EXAFS) technique, however, is ideally suited to detect small changes in local structure. We, therefore, carried out EXAFS experiments on both $PrRu_4P_{12}$ and $PrOs_4P_{12}$, because $PrOs_4P_{12}$ is a close structural relative of $PrRu_4P_{12}$, but is a metal below room temperature. Our data clearly show that a structural distortion of an unexpected nature accompanies the MI transition in $PrRu_4P_{12}$.

EXAFS data at the Pr L_{III} edge, Os L_{III} edge, and the Ru K edge were collected as a function of temperature at beam line 20-BM at the Advanced Photon Source (APS). Single crystal samples were ground into very fine powders and brushed onto scotch tape for the measurements (particle size $\sim$10 μm). Energy-space data were reduced using standard procedures [10,11] and the resulting k-space data were Fourier transformed to r space yielding peaks that correspond to different atomic shells. By fitting each r-space peak to a theoretical function calculated using the FEFF8 program [12] plus a Gaussian pair distribution function, we extracted the peak widths σ and peak distances r. σ provides quantitative information about the local distortions, including thermal vibration and static distortion, of a particular atomic shell.

Fits to the Pr L_{III}-edge r-space data were performed for the first two atomic shells [Pr-P and Pr-Ru(Os)]. Figure 1(a) shows the fit result to the 25 K data for $PrRu_4P_{12}$ as an example of the fit quality. Since the filler atoms stay in a relatively large cage in the filled skutterudites, it is possible that the filler atoms might be displaced to an off-center position. Indeed, for $PrOs_4Sb_{12}$, the larger value of σ^2 at low temperatures indicated additional distortions which could be caused by a small Pr off-center

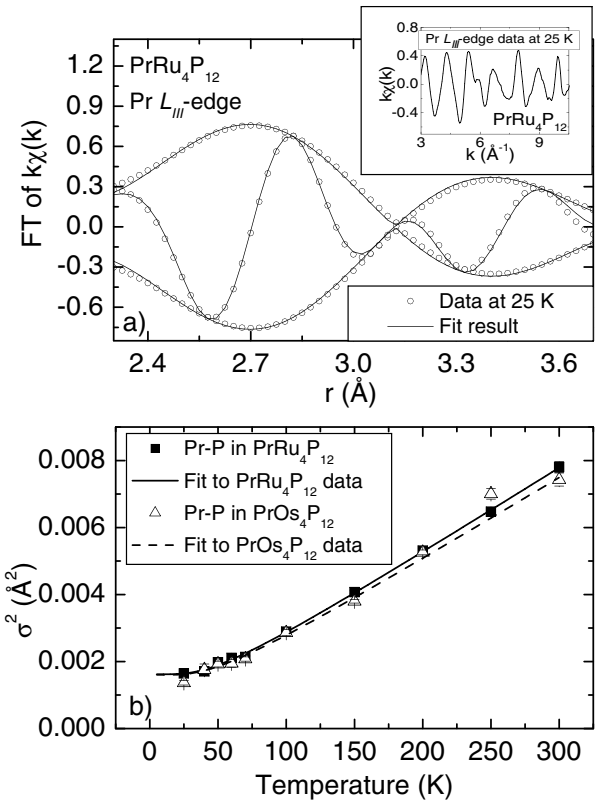

FIG. 1. (a) Pr L_{III}-edge r-space data for $PrRu_4P_{12}$ at 25 K and the fit result. The Fourier transform range is from 3.0 to 10.5 $Å^{-1}$, with 0.3 $Å^{-1}$ Gaussian broadening. The fit range is from 2.3 to 3.7 Å. The high frequency curve inside the envelope is the real part of the Fourier transform (FT_R). The envelope is defined as $\pm\sqrt{FT_R^2 + FT_I^2}$, where FT_I is the imaginary part of the transform. There is a well-defined EXAFS phase shift for each peak, consequently the nearest Pr-P peak occurs at ~2.7 Å and the Pr-Ru peak is at ~3.4 Å. The inset displays Pr L_{III}-edge k-space data at 25 K as an example to show the quality of the EXAFS data. (b) The temperature dependent σ^2 obtained from fits for the Pr-P bond in $PrRu_4P_{12}$ and $PrOs_4P_{12}$ samples. The results of fitting σ^2 vs T to an Einstein model for each sample are also plotted.

displacement [13]. We, therefore, suspected that the MI transition in $PrRu_4P_{12}$ might be due to a Pr off-center displacement at low temperatures. However, σ^2 for the Pr-P bonds, extracted from the fits [Fig. 1(b)] for $PrRu_4P_{12}$ and $PrOs_4P_{12}$, show no obvious anomalies as the temperature drops below 60 K. The rattling of the filler atoms is considered to be a localized vibration and, therefore, should be consistent with an Einstein model [14]. As shown in Fig. 1(b), both sets of data can be very well fit to an Einstein model with no obvious deviation across T_{MI}. In fact, the static distortions, reduced masses, and Einstein temperatures obtained in $PrRu_4P_{12}$ and $PrOs_4P_{12}$ are very similar, which suggest that the Pr local structure is essentially the same in both samples [static distortions ~0.000 03(5) $Å^2$; reduced masses ~112(5) g/mol; Einstein temperatures ~130(3) K]. Thus, we have no evidence for Pr off-center displacement in $PrRu_4P_{12}$ at any temperature, and consequently conclude that Pr displacement cannot be the origin of the MI transition in this material.

We now compare the Ru K-edge data and the Os L_{III}-edge data for the two materials. Figure 2 plots the r-space data and the fit result at the lowest temperatures for each edge. The four nearest atomic shells [Ru(Os)-P, Ru(Os)-Pr, second Ru(Os)-P, and Ru(Os)-Ru(Os)] were used to fit the data. To account for a possible interference between further multiscattering peaks and the Ru(Os)-Ru(Os) peak, two additional multiscattering peaks at longer distances with small amplitudes were also included in the fit.

Figure 3 shows the temperature dependence of σ^2 together with fits of $\sigma^2(T)$ to a Debye model for the Ru(Os)-P and Ru(Os)-Ru(Os) atom pairs. For the Ru-P and Os-P bonds, no anomaly in $\sigma^2(T)$ was found across T_{MI}. The high Debye temperatures obtained for these two bonds ($\Theta_D = 690$ K for Ru-P and 720 K for Os-P) suggest that the Ru-P and Os-P bonds are rather strong, making the RuP_6 and OsP_6 octahedra in $PrRu_4P_{12}$ and $PrOs_4P_{12}$ rigid

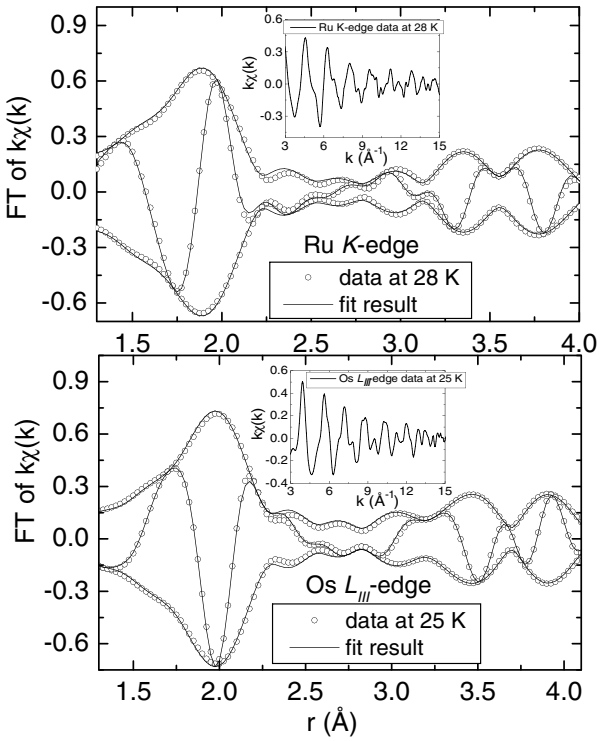

FIG. 2. A plot of the Ru K-edge and the Os L_{III}-edge r-space data at 28 and 25 K along with the fit result for $PrRu_4P_{12}$ and $PrOs_4P_{12}$, respectively. The Fourier transform range is from 3.0 to 15.0 $Å^{-1}$, with 0.3 $Å^{-1}$ Gaussian broadening for both edges. The fit range is from 1.2 to 4.0 Å for the Ru K-edge data, while it is 1.2 to 4.1 Å for the Os L_{III}-edge data. The Ru-P peak is at ~1.8 Å and the Ru-Ru peak is at ~3.8 Å, while the Os-P peak is at ~2.0 Å and the Os-Os peak is at ~3.9 Å. The insets in both panels plot the k-space data for each edge, respectively, to show the quality of the EXAFS data.

units. The most interesting feature in this figure is that the σ^2 of the Ru-Ru pair starts to increase as T drops below 60 K ($\approx T_{\mathrm{MI}}$). If thermal vibrations dominated the broadening, σ^2 should gradually decrease as T decreases, saturating at the zero-point-motion value. The σ^2 for the Os-Os atom pair indeed follows this trend ($\Theta_D \approx 370$ K). However, the increase in σ^2 for the Ru-Ru pair at low temperatures clearly indicates that an extra distortion other than thermal vibration exists below 60 K in $PrRu_4P_{12}$. Fitting the Ru-Ru σ^2 data from 70 to 300 K yields Θ_D of $\sim$398 K with zero static distortion (the solid curve in Fig. 3). Despite the excellent agreement with the $T \geq 70$ K data, this fit yields a curve distinctly below the data for $T \leq 60$ K. Attempts to fit the Ru-Ru data at all temperatures to a single Debye model plus a small static distortion (the dotted curve in Fig. 3) yields a Θ_D of 413 K and static distortion of 0.000 18 Å^2. This model, however, fails to give a good fit to either the high- or low-temperature data. Thus there must be an extra Ru-Ru distortion at temperatures below 60 K.

We now discuss the origin of this Ru-Ru distortion. In the undistorted lattice, all Ru-Ru distances are the same, so that any small expansion or contraction of the Ru framework that does not break this degeneracy cannot lead to a larger σ^2 for the Ru-Ru peak. Thus, this extra distortion found for the Ru-Ru pair at low temperatures must come from a Ru displacement that breaks the degeneracy of the

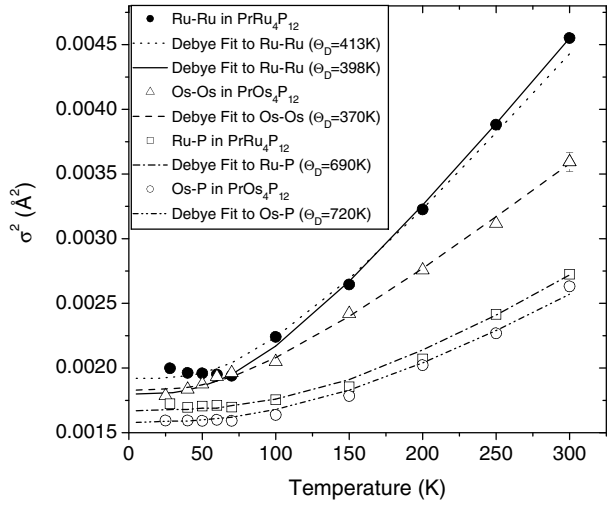

FIG. 3. σ^2 vs temperature for the Ru(Os)-P, Ru(Os)-Ru(Os) atom pairs obtained from the Ru K-edge and the Os L_{III}-edge EXAFS data for $PrRu_4P_{12}$ and $PrOs_4P_{12}$, respectively. The Debye model fit to each set of data is also shown in the figure. For the Ru-Ru pair (solid circles), σ^2 increases below 60 K; here two Debye models are used: the dotted line is the fit to the data points at all temperatures and yields Θ_D of 413 K; the solid line is the fit result to the data points for temperatures between 70 and 300 K, and gives Θ_D of 398 K. The relative error bar for each data point, which is not shown, is smaller than the symbol size, except for one data point indicated in the figure. The error for the Debye temperature is $\sim$20 K.

Ru-Ru distance. Lee *et al.* proposed that an $Im\bar{3}$ to $Pm\bar{3}$ phase transition is the origin of the MI transition in $PrRu_4P_{12}$ [5]. Because of a (1, 1, 1) Ru distortion, the Ru sublattices then have two different sizes in the $Pm\bar{3}$ phase. This splits the six nearest Ru-Ru atom pairs in the $Im\bar{3}$ phase into three long and three short pairs, which could produce an extra broadening of the Ru-Ru peak in the EXAFS r-space spectra. Although the low-T $Pmmm$ phase suggested by Curnoe *et al.* changes the cubic Ru sublattice to tetragonal and also creates Ru-Ru distortion [6,7], recent inelastic neutron scattering measurements show a Γ_1 ground state for Pr^{3+} in $PrRu_4P_{12}$ [15], indicating that the assumption of a Γ_3 ground state in Curnoe's theory is not correct. Furthermore, the number of transitions of excited crystal field levels observed in the inelastic neutron scattering experiments below T_{MI} are consistent with the two inequivalent Pr sites in the $Pm\bar{3}$ phase. Therefore, the possibility of the low-T $Pmmm$ phase can be excluded.

To test the $Pm\bar{3}$ model, we then fit the Ru-Ru peak in the EXAFS data with two Ru-Ru peaks. In this new fit, the number of neighbors was again fixed and the amplitude ratio of the two Ru-Ru peaks was set to be 1:1, each with a degeneracy of three. Also, the σ parameters for these two peaks were set equal, because the difference in the pair distances must be very small. Thus, only the Ru-Ru atom distances were allowed to change independently. As shown in Fig. 4(a), the low-temperature σ^2 from the double-peak model are now lowered and very consistent with the $\Theta_D = 398$ K Debye model which was used to fit the data from 70 to 300 K in the single-peak model. Note that for a single data trace, EXAFS analysis normally cannot resolve two peaks split by a small distance, because the fitting quality will be comparable for both a single-peak and a double-peak fit; however, both methods would show an overall increase in disorder compared to an unsplit peak. The excess broadening observed in many traces for $T < 60$ K from the single-peak fit is clearly inconsistent with thermal vibrations. This provides an additional constraint; if thermal vibrations cannot explain the increased disorder (and random disorder should not change at these temperatures), then the peak must have split from a phase transition. The resulting double-peak fit yields much more reasonable values of σ^2 below T_{MI}. Thus, we can conclude that the model with two different Ru-Ru distances is a better interpretation to our EXAFS data over a range of temperatures at low T.

The Ru-Ru peak distances obtained from the two fits (open circles and open squares) are also plotted in Fig. 4(b). The double-peak fit displays two Ru-Ru distances below T_{MI}, which are separated by about 0.022–0.030 Å. This value is consistent with recently obtained low-temperature synchrotron x-ray diffraction results [9]. The result of the double-peak fit is clearly consistent with a $Pm\bar{3}$ space group for $T \leq T_{\mathrm{MI}}$. Above T_{MI}, the two Ru-Ru peaks collapse back together in these fits, confirming a high-temperature $Im\bar{3}$ phase.

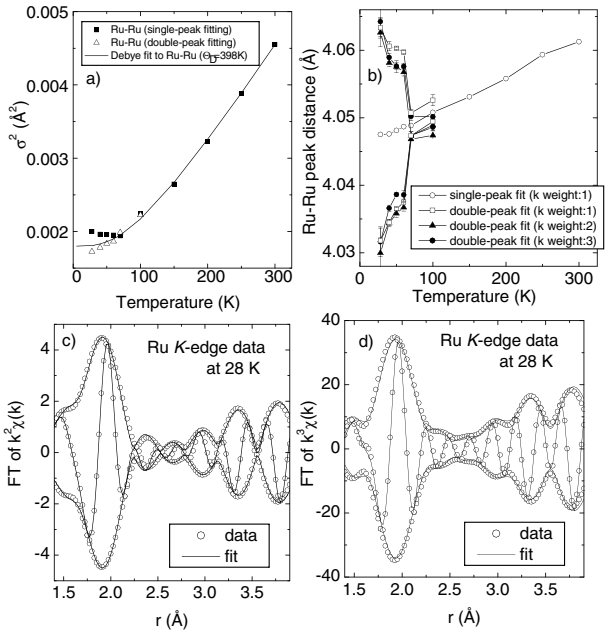

FIG. 4. (a) σ^2 of the Ru-Ru atom pair obtained from the original single Ru-Ru peak fit and the double Ru-Ru peak fit (with k weighting of 1) as well as the $\Theta_D = 398$ K Debye model. (b) The Ru-Ru peak distances obtained from the single-peak fit (k weighting of 1) and double-peak fits with k weightings of 1, 2, and 3. The error bars for all σ^2 data and the peak distance in the single-peak fit are smaller than the symbol size and, therefore, not shown. (c),(d) The fit results to data with k weightings of 2 and 3.

Fits to the data with different k weightings, $k^2\chi(k)$ and $k^3\chi(k)$, were also carried out to check the consistency of the double-peak fit result. As shown in Fig. 4(b), the bond lengths obtained from all fits show a similar jump between 60 and 70 K. This further confirms the validity of the fit result to the Fourier transform of $k\chi(k)$ data. Figures 4(c) and 4(d) show the fit results to data with two higher k weightings. The values of σ^2 obtained from fits with k^2 and k^3 weightings are very similar to those from the fit using k weighting of 1, which are not shown.

As pointed out earlier, because the RuP_6 octahedra are quite rigid units forming a corner-shared framework, a slight rotation, plus a tiny displacement, of the RuP_6 octahedra is needed to produce the observed Ru displacement. This inevitably leads to tiny correlated P displacements. However, because these P displacements are not principally along the radial directions of the Pr-P bonds, the subsequent Pr-P bond-length variations are too small to be observed in EXAFS [Fig. 1(b)].

Our EXAFS data clearly show that the MI transition in $PrRu_4P_{12}$ is associated with small correlated Ru and P displacements. Such atomic displacements may open a band gap at the Fermi surface, leading to semiconducting (insulating) behavior at low temperatures. A band structure calculation by Harima *et al.* indeed showed that very small P displacements can introduce a band gap in $PrRu_4P_{12}$ [8]. However, possible Ru displacements were not considered in that work. Thus, future theoretical calculations need to consider correlated displacements of Ru and P caused by a rotation/displacement of the RuP_6 octahedra.

We also note that recent inelastic neutron scattering experiments of $PrRu_4P_{12}$ have been interpreted [15] as evidence for a charge-density wave produced by strong $4f$ hybridization. Our results may help to illuminate this issue. The local-distortion-induced MI transition in $PrRu_4P_{12}$ may also be related to the semiconducting behavior observed in other phosphide skutterudites, such as $CeRu_4P_{12}$ and $CeFe_4P_{12}$. In this regard, the estimated static contribution to σ^2 for the Ru-Ru atom pair from the Ru K-edge data for $CeRu_4P_{12}$ is about 0.000 93 Å^2 at all temperatures [16]; assuming a distortion of the Ru positions, this corresponds to a Ru displacement $\sim$0.03 Å ($\sqrt{\sigma^2_{\text{static}}}$). A similar static distortion for the Fe-Fe atom pair in $CeFe_4P_{12}$ was also inferred.

In summary, we present the first comprehensive local structure measurements of $PrRu_4P_{12}$. We find that a static Ru displacement is clearly associated with the MI transition in $PrRu_4P_{12}$, while the P displacements must be associated with the motion of the rigid RuP_6 octahedra. This Ru displacement found in $PrRu_4P_{12}$ suggests that the low-temperature phase in this material is likely to be $Pm\bar{3}$. This EXAFS experiment clearly illustrates the importance of correlating the effects of local distortions with the transport properties of the filled skutterudites.

This work was carried out under the auspices of the U.S. Department of Energy, Office of Science. The experiments were preformed at APS, which is funded by the DOE, Office of Sciences, Office of Basic Energy Sciences. Research at UCSD was supported by the U.S. Department of Energy under Grant No. FG02-04ER46105.

[1] G. P. Meisner *et al.*, J. Appl. Phys. **57**, 3073 (1985).
[2] I. Shirotani *et al.*, J. Solid State Chem. **142**, 146 (1999).
[3] C. Sekine *et al.*, Phys. Rev. Lett. **79**, 3218 (1997).
[4] C. H. Lee *et al.*, Phys. Rev. B **60**, 13 253 (1999).
[5] C. H. Lee *et al.*, J. Phys. Condens. Matter **13**, L45 (2001).
[6] S. H. Curnoe *et al.*, Physica (Amsterdam) **312B–313B**, 837 (2002).
[7] S. H. Curnoe *et al.*, J. Phys. Chem. Solids **63**, 1207 (2002).
[8] H. Harima *et al.*, Acta Phys. Pol. B **34**, 1189 (2003).
[9] C. H. Lee *et al.*, J. Magn. Magn. Mater. **272–276**, 426 (2004).
[10] G. G. Li, F. Bridges, and C. H. Booth, Phys. Rev. B **52**, 6332 (1995).
[11] F. Bridges, C. H. Booth, and G. G. Li, Physica (Amsterdam) **208B&209B**, 121 (1995).
[12] A. L. Ankudinov *et al.*, Phys. Rev. B **58**, 7565 (1998).
[13] D. Cao *et al.*, Phys. Rev. B **67**, 180511(R) (2003).
[14] V. Keppens *et al.*, Nature (London) **395**, 876 (1998).
[15] K. Iwasa *et al.* (to be published).
[16] D. Cao *et al.*, Phys. Rev. B, **70**, 094109 (2004).